RSC Advances

PAPER

View Article Online
View Journal | View Issue

Cite this: *RSC Adv.*, 2023, **13**, 24925

An efficient method to access spiro pseudoindoxyl ketones: evaluation of indoxyl and their *N*-benzylated derivatives for inhibition of the activity of monoamine oxidases†

Karuppaiah Perumal,[a] Jiseong Lee,[b] Sesuraj Babiola Annes,[a] Subburethinam Ramesh,*[a] T. M. Rangarajan,[c] Bijo Mathew[d] and Hoon Kim*[b]

Received 31st May 2023
Accepted 3rd August 2023

DOI: 10.1039/d3ra03641c

rsc.li/rsc-advances

A simple, metal-free approach was developed to obtain novel pseudoindoxyl derivatives. The reaction was mediated by *t*BuOK on tetrahydrocarbazole **8** in dimethyl sulfoxide (DMSO) at room temperature through the hydroxylation of the indole double bond and a subsequent pinacol-type rearrangement. Spiro pseudoindoxyl compounds and their *N*-benzylated derivatives were assessed for their inhibitory activities against monoamine oxidase (MAO) enzymes. Based on half-maximal inhibitory concentration (IC_{50}) values, 13 compounds were found to have higher inhibitory activity against MAO-B than against MAO-A. With regard to MAO-B inhibition, **11f** showed the best inhibitory activity, with an IC_{50} value of 1.44 μM, followed by **11h** (IC_{50} = 1.60 μM), **11j** (IC_{50} = 2.78 μM), **11d** (IC_{50} = 2.81 μM), and **11i** (IC_{50} = 3.02 μM). Compound **11f** was a competitive inhibitor with a K_i value of 0.51 ± 0.023 μM. In a reversibility experiment using dialysis, **11f** showed effective recovery of MAO-B inhibition similar to that of safinamide. These experiments suggested that **11f** was a potent, reversible, and competitive inhibitor of MAO-B activity.

Introduction

Many alkaloids and biologically active substances have spiro core heterocyclic structures.[1] Indole is an important heterocyclic core found in many natural products. The pseudoindoxyl sub-structural motif is a unique subgroup of the class of oxygenated indoles among the many alkaloids.[1] The pesudoindoxyl structure (especially one with a spiro quaternary C2 carbon center) is an essential skeleton of indole alkaloids. The pseudoindoxyl alkaloids are an excellent example of a 2,2-disubstitution of a pseudoindoxyl compound, which is a preferred entity because it is a vital part of many important chemical compounds.[2] Examples of characteristic natural products with different biological activities in these spiro pseudoindoxyl compounds include duocarmycin c1/b2, brevianamide A (**4**), (+)-aristotelone (**3**), and diketopiperazine (**7a**) (Fig. 1).[3]

Moreover, the extracts of leaves of *Mitragyna speciosa* and flowering plants of the Rubiaceae family contain alkaloids with diverse structural motifs such as indole, indolenine, and spiro pseudoindoxyl. The natural product mitragynine undergoes rearrangement into mitragynine pseudoinoxyl after oxidation at an indole site to form 7-hydroxymitragynine, and all of them show powerful pain-relieving (or analgesic) effects and opioid activity. The mitragynine pseudoindoxyl acts non-selectively on mu- and delta-opioid receptors.[2h,j] These opioids have shown neuroprotective effects against hypoxia–ischemia injury and have a modulatory effect on the regulation of neurotransmitter chemicals. Recently, the importance of opioids receptors in modulation of more complicated neurodegenerative diseases (*e.g.*, Alzheimer's disease (AD)) has been shown.[2j,k] The biological activity of these alkaloids has yet to be explored. Because of the affinity of these compounds with opioid receptors, we were interested in evaluating the role of the pseudoindoxyl core in neurodegenerative diseases by inhibiting some of their target enzymes, such as monoamine oxidases (MAOs).

Furthermore, in recent years, these compounds have been demonstrated to have fascinating roles in terms of bioactivity, materials research, and optoelectronic research (Fig. 1).[4–7] For example, the lipid droplets in the 3T3L1 cell line and fat deposits in zebrafish were strained using these pseudoindoxyl derivatives without apparent toxicity up to 100 mM.[4] Alkyne-linked 2,2-disubstituted pseudoindoxyl oligomers have been

[a]*Department of Chemistry, School of Chemical and Biotechnology, SASTRA Deemed University, Thanjavur 613 401, Tamil Nadu, India. E-mail: rameshsbdu@gmail.com*
[b]*Department of Pharmacy, Research Institute of Life Pharmaceutical Sciences, Sunchon National University, Suncheon 57922, Republic of Korea. E-mail: hoon@sunchon.ac.kr*
[c]*Department of Chemistry, Sri Venkateswara College, University of Delhi, New Delhi, India*
[d]*Department of Pharmaceutical Chemistry, Amrita School of Pharmacy, Amrita Vishwa Vidyapeetham, AIMS Health Sciences Campus, Kochi 682 041, India*

† Electronic supplementary information (ESI) available: ^1H, $^{13}C\{1H\}$ NMR and HRMS spectra of all compounds. See DOI: https://doi.org/10.1039/d3ra03641c

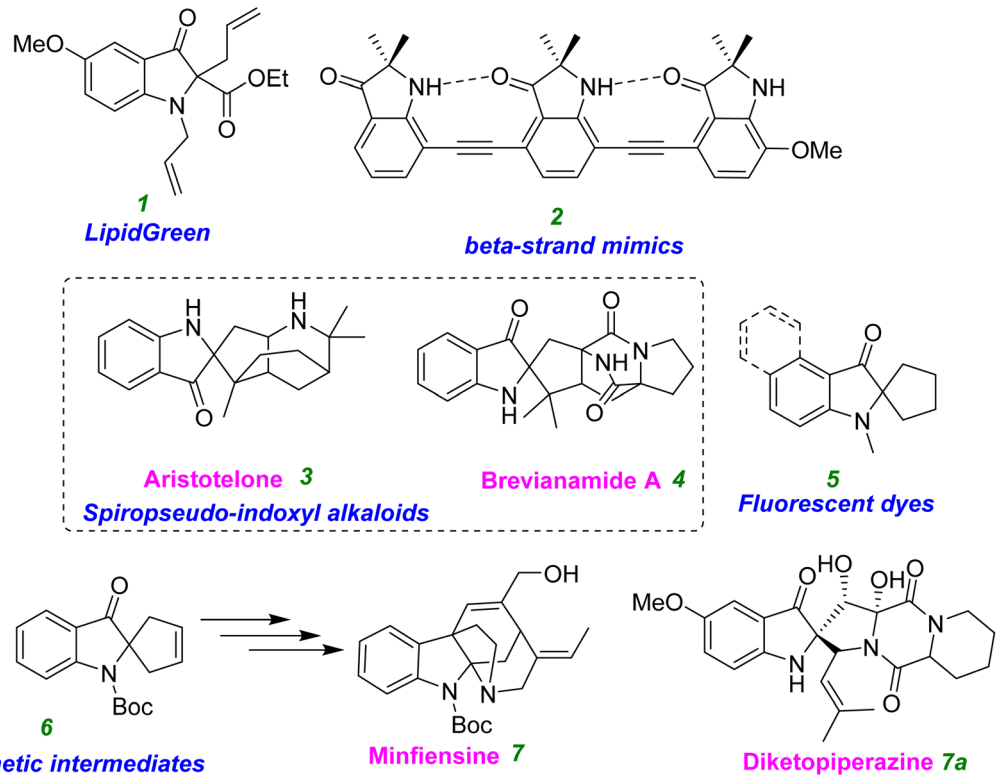

Fig. 1 Examples of important pseudoindoxyl derivatives.

identified as extended beta-strand mimics.[5] Four organic dye compounds generated from pseudoindoxylyl showed excellent photophysical characteristics.[6] A novel family of pseudoindoxyl compounds with a useful two-photon characteristic has been used for bioimaging and sensing studies.[7]

Therefore, the methodology in accessing the pseudoindoxyl core is of high interest and in demand. Significant effort has been invested in designing these crucial structures,[8] such as 8-desbromohinckdentine A.[1] A typical procedure involves the two-step process of hydroxylation using oxidants such as DMDO, mCPBA, HNO_2, and oxone, followed by a reaction in which the hydroxyl-imine is rearranged to produce a spiro compound (2,2-disubstituted pseudoindoxyl) using a strong acid or base[8a–k] (Scheme 1, eqn (a)). Several methods have been reported for accessing the pseudoindoxyl core. Glorius *et al.* described a highly enantioselective NHC-catalyzed annulation method for synthesizing pseudoindoxyl derivatives from unsaturated aldehydes and aurones (Scheme 1, eqn (b)).[9a] In contrast, Sorensen described a two-step process for the Houben–Hoesch cyclization and Ugi reaction utilizing imines and isocyanides (Scheme 1, eqn (c)).[9b] Allenamides were activated by Rossi *et al.* using a gold catalyst, and the resultant furan ring-opening reaction led to the production of pseudoindoxyl derivatives (Scheme 1, eqn (d)).[9d] Xiao *et al.* reported on visible-light hydroxylation and cyclization catalyzed by $Ru(bpy)_3Cl_2 \cdot 6H_2O$.[9f] Stepwise oxidation followed by a rearrangement reaction, stoichiometric oxidants,[8] as well as the need for transition metals,[9] expensive metal photocatalysts,[9f] and high reaction temperatures are the drawbacks of these methodologies.[8,9] As a result, alternative synthetic routes to the spiro-pseudoindoxyl structure must be developed using a mild and efficient approach.

MAOs are necessary for the management of brain function. MAOs oxidize monoamines to produce ammonia, aldehydes, and hydrogen peroxide as byproducts. Excessive production of these byproducts of monoamine metabolism generate free radicals, which lead to apoptosis and give rise to several neurodegenerative disorders, such as AD and Parkinson's disease (PD).[10,11] MAO inhibitors are employed as co-adjuvants to treat neurodegenerative illnesses (selective inhibitors of MAO-B) or antidepressants (selective inhibitors of MAO-A). Such studies may be of significant interest because of the crucial role of MAOs in regulating brain processes, mood, cognitive activity, and monoamine catabolism.[12,13] The US Food and Drug Administration-approved MAO-B inhibitor selegiline binds irreversibly to the enzyme target.[14] This action can lead to target disruption, a prolonged duration of action, and poor pharmacokinetic profiles.[15–17] The lack of alternatives, combined with the limitations of existing drugs, has led to a new trend in the design and development of molecules in the reversible-binding mode. Many research teams have explored the potential of MAO-B inhibition of indole derivatives and a bicyclic heteroaromatic nucleus.[18–20] However, the role of the natural products spiro pseudoindoxyls in neurodegenerative diseases have not been explored. We were able to develop a simple and straightforward methodology for accessing the pseudoindoxyl core of natural products. Hence, we were interested in evaluating the MAO inhibitory effects of the pseudoindoxyl motif and its *N*-benzyl derivatives.

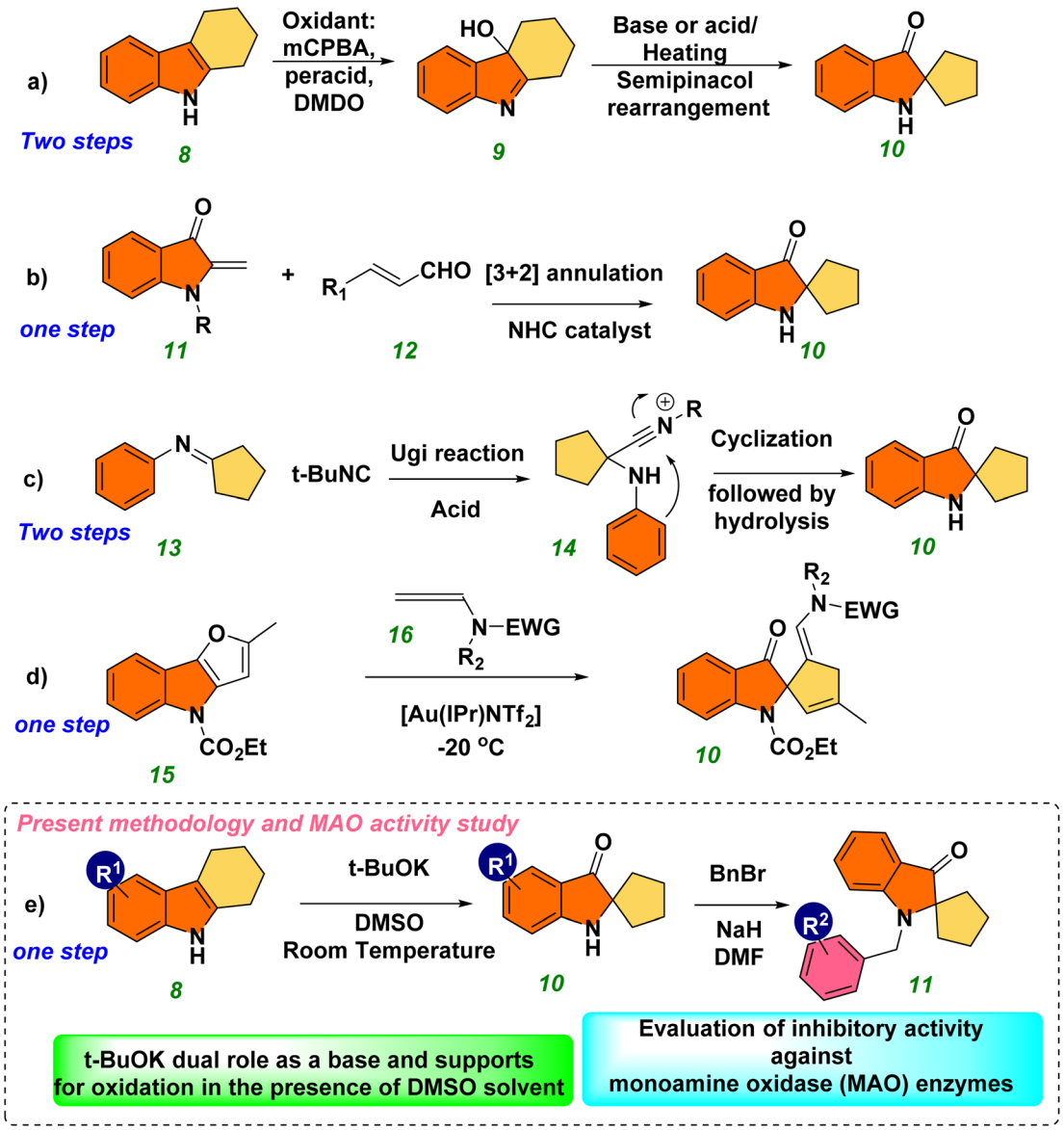

Scheme 1 Synthetic approaches for spiro pseudoindoxyl derivatives.

Results and discussion

Chemistry

The development of cheaper and more environmentally friendly synthetic-chemical approaches is highly desirable. In this context, we developed a metal-free, base-promoted synthesis of heterocyclic spiro compounds through 3-hydroxylation of tetrahydro carbazole. This novel approach incorporates a metal-free, one-pot synthesis under mild reaction conditions with a cheap base (tBuOK). Tetrahydrocarbazole (THC) was used as a precursor for synthesizing spiro ketones, which were obtained readily using Fisher indole synthesis. The MAO-inhibitory profiles of these novel synthesized spiro-based indole derivatives were evaluated (Scheme 1, eqn (e)).

Tetrahydrocarbazole THC (**8a**)[21] (1 equiv), NaOH (1.5 equivalent), and a solvent combination (water–DMSO) were used for the initial optimization study, and the final product **10a** was obtained at 40% yield without formation of the intermediate **9a**. The structure of compound **10a** was determined unambiguously by ^{1}H, ^{13}C, and high-resolution mass spectrometry (HRMS) (ESI†). The aliphatic methylene ($-CH_2$) protons shifted from their original positions in compound **8a** owing to formation of a spiro ring in compound **10a**. The chemical shift was most likely caused by the more strained structure and presence of a carbonyl group at C3 in compound **10a**, which caused the chemically equivalent $-CH_2$ protons to become non-equivalent 2.11–2.05 (2H, m), 2.00–1.93 (2H, m), 1.88–1.83 (2H, m), and 1.75–1.70 (2H, m). The broad singlet at 5.00 ppm indicated the presence of a free-NH group. The deshielding behavior exhibited by the aromatic ring appeared as one doublet, one triplet, and one multiplet at the corresponding frequencies of 7.61, 7.43, and ~6.8 ppm, respectively. The overlap of a doublet and

Table 1 Optimization condition for the synthesis of spiro pseudoindoxyl derivative **10a**[a]

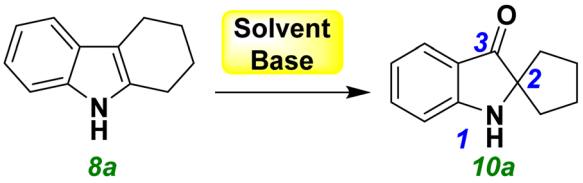

Entry	Base	Solvent	Yield[b] (%)
1[c]	NaOH (1.5 equiv.)	H_2O + DMSO	40
2[c]	NaOH (1.5 equiv.)	H_2O + DMF	38
3[c]	K_2CO_3 (1.5 equiv.)	DMSO	40
4	K_2CO_3 (1.5 equiv.)	DMSO	47
5	Cs_2CO_3 (1.5 equiv.)	DMSO	52
6	*t*-BuOK (1.5 equiv.)	DMSO	68
7[c]	*t*-BuOK (1.5 equiv.)	DMSO	32
8[d]	*t*-BuOK (1.5 equiv.)	DMSO	69
9[e]	*t*-BuOK (1.5 equiv.)	DMSO	60
10[f]	*t*-BuOK (1.5 equiv.)	DMSO	41
11[g]	*t*-BuOK (1.5 equiv.)	DMF	36

[a] Unless noted otherwise, base 1.5 equiv., DMSO 1 mL, 24 h, N_2 atmosphere. [b] Isolated yield. [c] Open air. [d] Under O_2 atm, 2.5 h. [e] Under dark condition. [f] 1 h. [g] 50 °C, 2 h.

a triplet caused the appearance of a multiplet. The signal at 205.20 ppm in the ^{13}C nuclear magnetic resonance (NMR) spectrum of $CDCl_3$ at 75 MHz demonstrated the presence of ketone functionality. The less intense peaks at 159.96, 120.58, and 74.64 ppm were responsible for quaternary carbons in **10a**. The peak at 74.64 ppm was highly significant and revealed a newly formed quaternary spiro carbon. Aromatic deshielded carbons were represented by peaks at 136.89, 124.54, 118.65, and 112.22 ppm. Aliphatic methylene carbons were indicated by peaks at 38.01 and 25.41°. HRMS (*m*/*z*) analysis verified the mass of **10a**. Further optimization of reaction conditions using a water–DMF solvent mixture reduced the yield to 38% (Table 1, entries 1 and 2). Use of a K_2CO_3 base (Table 1, entries 3 and 4), with or without an inert atmosphere, did not significantly affect the yield of the spiro compound **10a**. The yield did not increase considerably upon addition of Cs_2CO_3 (Table 1, entry 5). The base *t*-BuOK facilitated the reaction in an N_2 environment, improving the yield of spiro compound **10a** significantly (68%) in 24 h (Table 1, entry 6). With this successful attempt, reactions were also carried out under air and an oxygen-containing atmosphere, and afforded 32% and 69% yields, respectively, of the spiro compound **10a** (Table 1, entries 7 and 8). The results stated above indicated that the base was quenched in open air owing to moisture and that the presence of oxygen was crucial for the reaction because the reaction was completed within 2.5 h in an oxygen balloon. We repeated the reaction in the absence of light to establish the importance of visible light, but a discernible response was not observed (Table 1, entry 9). The conversion of the starting material THC **8a** was affected by reducing the reaction time to 1 h (Table 1, entry 10). While heating the reaction mixture with DMF at 50 °C, several spots in thin-layer chromatography (TLC) were seen (Table 1, entry 11). The optimized conditions for the synthesis of spiro pseudoindoxyl compound **10a** were, therefore, set at 1 equiv. of THC **8a** in DMSO solvent and 1.5 equiv. of *t*-BuOK under an O_2 atmosphere for 2.5 h (Table 1, entry 8).

The scope and limitations of synthesizing spiro pseudoindoxyl derivatives were examined under ideal conditions (Scheme 2). Spiro pseudoindoxyl derivatives **10a–10j** were synthesized using various amounts of THC (**8a–8j**),[21] and the isolated products were characterized by NMR and HRMS. The yield of product **10b** was not affected significantly by the electron-donating group at the R^1 position of THC (**8b**). The compounds with chloro- and bromo-substitution at the R^1 position (**8c** and **8d**) produced the corresponding spiro compounds (**10c** and **10d**) in better yields than the fluoro-substituted THC **8e**, among the halogen groups (**8c–8e**) in the R^1 position of THC. The yield of compound **10f** was reduced marginally, whereas the yield of the electron-withdrawing bromo-substituted compound **10g** was lower than that of compound **10f**. The methyl substitution at R^3 had little effect on the yield of product **10h**, whereas the bromo substitution at R^3 had a considerable effect on the yield of product **10i**. The disubstituted compound (**8j**) yielded spiro compound **10j** in modest yield.

Next, we planned to benzylate the nitrogen group of spiro pseudoindoxyl compound **10a**. When benzyl bromide **19a** was used to treat a mixture of spiro pseudoindoxy compounds **10a** and DMF in the presence of NaH and nitrogen gas, a good-to-outstanding yield of *N*-benzylated spiro pseudoindoxyl compounds **11a** was obtained (Scheme 3). By adjusting benzyl bromides (**19b–19g**) and spiro pseudoindoxyl compounds**10b–10e**, the scope of the reaction was determined (**11b–11k**). Benzylation of spiro compound **10** with an electron-donating compound (–CH_3, **10b**), electron-withdrawing compounds –Cl (**10c**), –Br (**10d**), –F (**10e**), and unsubstituted compound **10a** afforded average-to-high yields of benzylated compounds **11a–11e**. Compared with electron-donating and other halogen substituents, –F affected the benzylation pathway because it could reduce the nucleophilicity of the ring. We also synthesized several additional derivatives utilizing various benzyl bromides **19b–19g** that were tested. Except for the –CN group **19d**, which had a strong withdrawing character, all substitutes for **19** afforded good yields (**11f**, **11g**, **11i**, **11j**); this was because **19d** reduced the stability of the phenylmethylium ion during the benzylation reaction. Owing to the *ortho* effect, the yield of product **11k** decreased when the benzyl ring (*o*-Br, **19g**) was ortho-substituted. A probable mechanistic route for the metal-free hydroxylation cascade reaction based on the substituent impact and reactivity of the substrate was postulated. Following that, we attempted a gram-scale synthesis with compound **8a** under standard reaction conditions, which yielded 69% of the product **10a** (eqn (1), Scheme 4). Under standard reaction conditions of the benzylation reaction, compounds **10a** and benzyl bromide provided compound **11a** in an excellent yield of 91% (eqn (2), Scheme 4).

We undertook some control experiments to ascertain the reaction mechanism. When we carried out a reaction with **17** under optimized conditions, the expected product **17a** was not

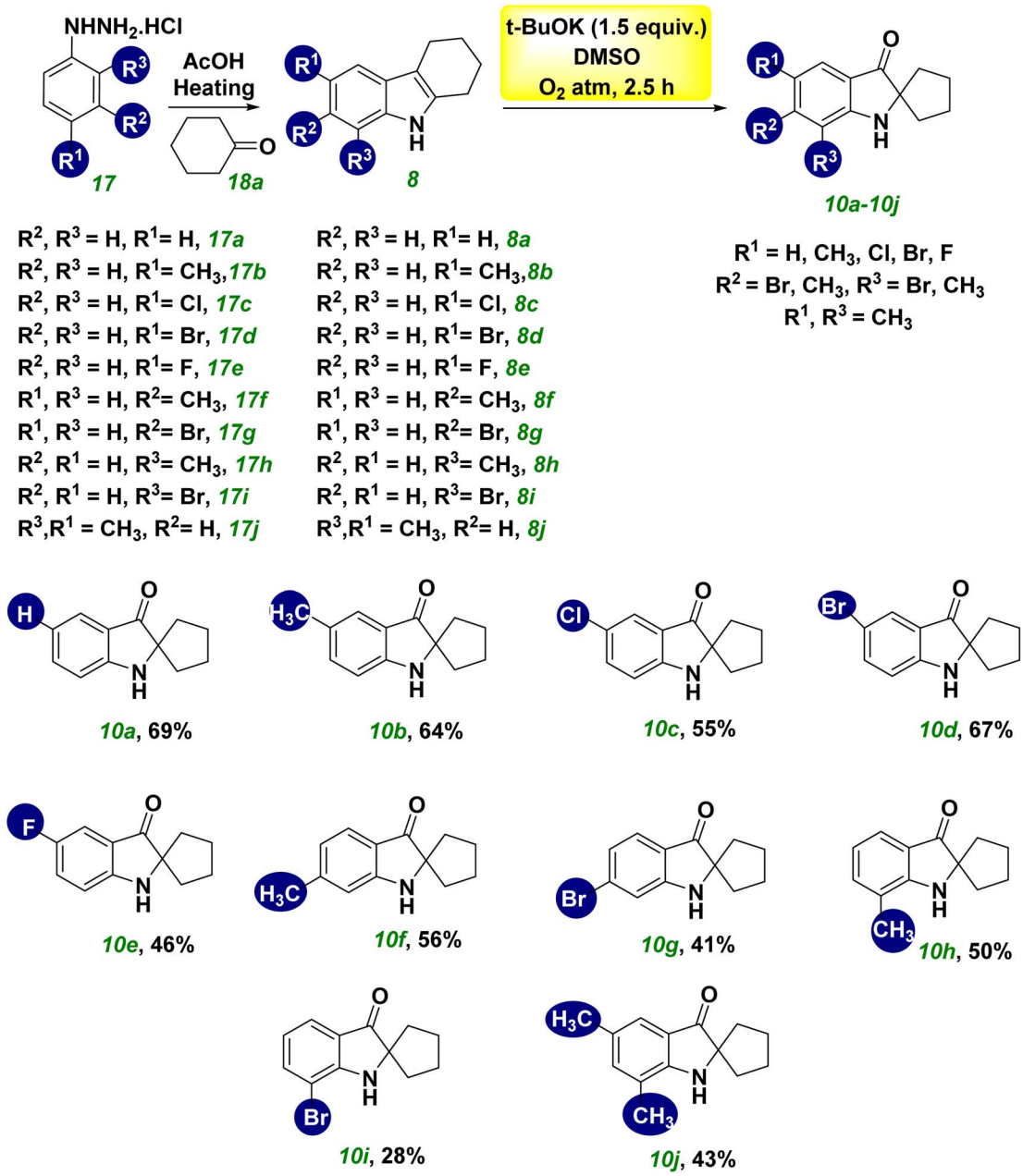

Scheme 2 Scope of the synthesis of spiro pseudoindoxyl derivatives 10a–10j.

obtained. This result indicated the importance of the secondary cyclic amine system compared with the tertiary amine (eqn (1), Scheme 5). To ascertain if any radical path was involved in the reaction conditions, C–H hydroxylation was carried out with the radical quencher TEMPO (2 equivalent). However, we did not find a decrement in the yield because 69% of the product was obtained (eqn (2), Scheme 5). Compound **8a** was treated with **19** under standard conditions, but product **11a** was not obtained. This result clearly indicated that the deprotonation followed by an S_N2 reaction with **19a** was faster than the hydroxylation reaction because **11a** product was not formed (eqn (3), Scheme 5).

Based on the substrate scope, control experiments, and the literature,[28] we proposed a reaction mechanism for formation of the spiro ring (Scheme 6). For the initial formal hydroxylation of THC **8a** using DMSO in the presence of *t*-BuOk, the base removed a proton from THC **8a** and generated anion **9a.** This anion was stabilized by the enamine system, and attacked oxygen molecules. Subsequently, the newly formed superoxide anion **9c** abstracted a proton from **8a** and generated **9d.** Further transformation of **9d** into **9e** facilitated an intra-molecular pinacol-type rearrangement for formation of the **9f** intermediate. Upon proton transfer on **9f**, compound **10a** was obtained readily. A benzylation reaction on **10a** followed deprotonation of **10a** by NaH as well as a S_N2 nucleophilic reaction with **19a**, and resulted in the product **11a**.

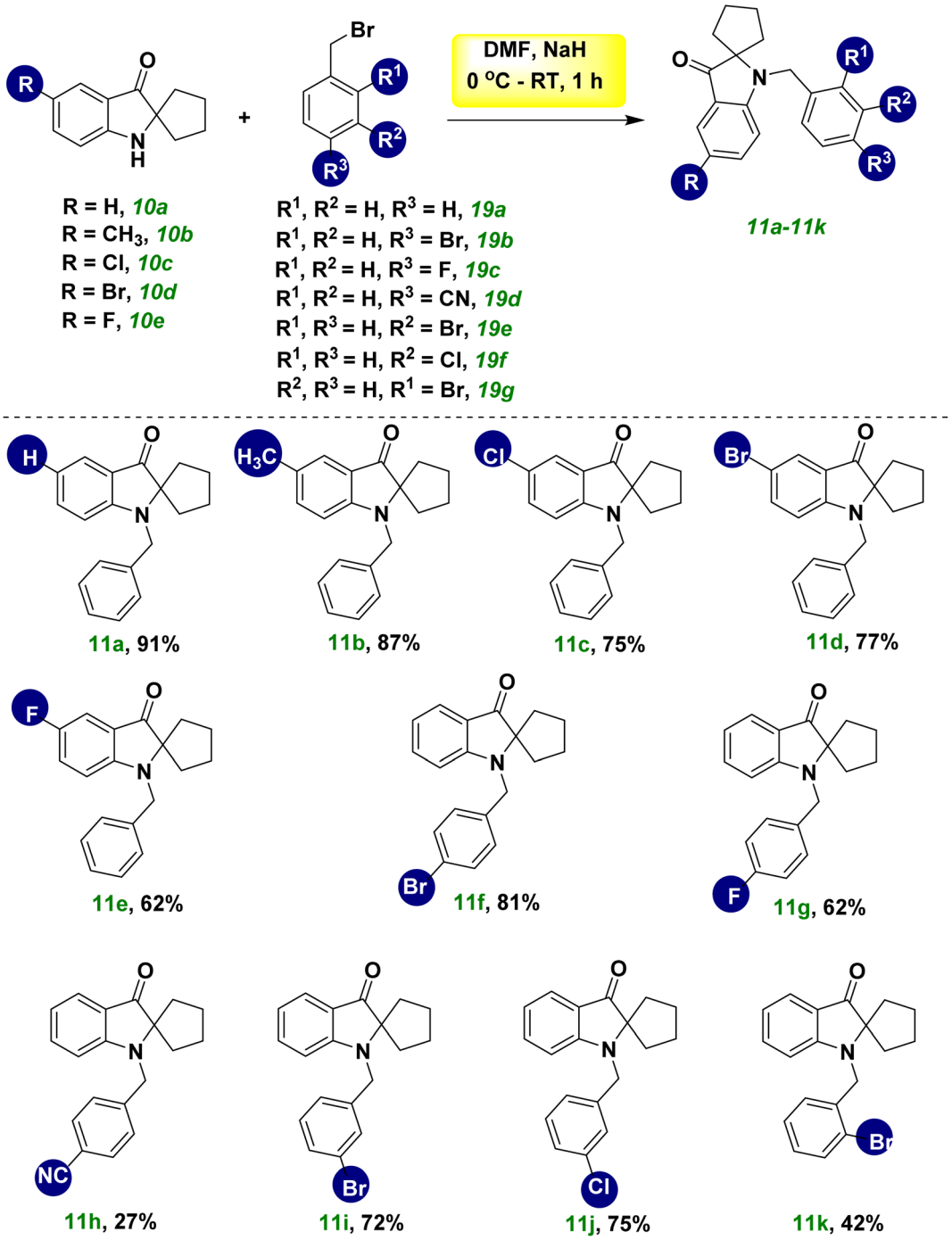

Scheme 3 Synthesis of various benzylated-spiro pseudoindoxyl derivatives **11a–11k**.

Biochemistry

Inhibition studies of MAO-A and MAO-B. At a concentration of 10 μM, eight compounds showed a low residual activity of <50% for MAO-B, whereas three compounds showed a low residual activity of <50% for MAO-A (Table 2). Compound **11f** had a half-maximal inhibitory concentration (IC_{50}) of 1.44 μM, showing the greatest inhibitory potential against MAO-B, followed by compounds **11h** ($IC_{50} = 1.60$ μM), **11j** ($IC_{50} = 2.78$ μM), **11d** ($IC_{50} = 2.81$ μM), and **11i** ($IC_{50} = 3.02$ μM). In terms of MAO-A inhibition, **11i** had the highest inhibitory activity, and the IC_{50} value was 5.58 μM (Table 2). Among these compounds, **11h** had the highest selectivity index (SI) value (14.01), followed by **11f** (11.91) for MAO-B.

Spiro-compounds were classified into two types. Modified isatin compounds were divided into two groups based on the absence (**10a–10e**) or presence (**11a–11k**) of a separate benzyl ring. In most cases, compounds with a benzyl ring showed greater inhibition of MAO-B activity. If the substituent was

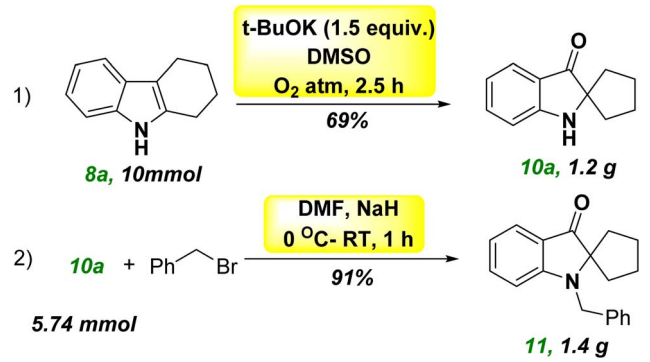

Scheme 4 Gram-scale synthesis.

present at the *meta*- or *para*-sites of the benzyl ring (**11f–11k**), low IC_{50} values were observed, except for **11g**. In addition, if the halogen substituent was bound to the isatin ring, good inhibitory activity was observed in the order –Br (**11d**) > –Cl (**11c**) > –F (**11e**). When comparing compounds in which -Br was bonded to the *N*-benzyl ring, compounds **11d**, **11f**, and **11i**, except for **11k**, showed good inhibition of MAO-B activity.

Enzyme kinetics. Enzyme kinetics and inhibition studies were undertaken using five substrate concentrations and three inhibitor concentrations of **11f**. In the Lineweaver–Burk plot, **11f** showed competitive inhibition of MAO-B (Fig. 2A). Secondary plots revealed a K_i value of 0.51 ± 0.023 μM (Fig. 2B). These results suggested that **11f** acted as a competitive inhibitor of MAO-B.

Reversibility studies. The reversibility of MAO-B inhibition by **11f** was analyzed by dialysis after 30 min of pre-incubation. The concentration of compound **11f** used was 2-times the IC_{50} value (2.88 μM). Recovery patterns were compared using undialyzed (A_U) and dialyzed (A_D) relative activities. Inhibition of MAO-B by compound **11f** recovered from 24.40% to 75.00% (Fig. 3). The recovery value of compounds was similar to that of safinamide (reversible type, from 14.41% to 89.68%), and could be distinguished from pargyline (irreversible type, 20.00% to 26.72%). These results suggested that **11f** was a reversible inhibitor of MAO-B.

Conclusions

We devised a novel, metal-free protocol for easy access to spiro pseudoindoxyl ketones. The reaction proceeded in one pot at room temperature with a cheap *t*-BuOK base under an oxygen atmosphere in DMSO. The methodology afforded products with different substituted THC values in moderate-to-good yields. The electron-releasing group on the benzene ring afforded products with good yields, whereas electron-withdrawing substituents, such as F and **10e**, generated moderate yields. To evaluate the cascade process, several 2-spirocyclo-3-oxindoles were synthesized. The reaction progressed through hydroxylation of the carbazole double bond and a subsequent intramolecular pinacol–pinacolone-type rearrangement. Then, the spiro compounds were transformed into their *N*-benzylated derivatives, and both series were evaluated for MAO inhibition. The non-benzylated spiro derivatives **10a–10e** did not exhibit good inhibition of MAO activity. In contrast, all *N*-benzylated spiro derivatives exhibited good inhibition of MAO-B activity (IC_{50} = 1.60–9.33 μM), except for **11a**, **11g**, and **11k**. Among them, compounds **11f** and **11h** exhibited the best inhibitory effects, with the IC_{50} value of 1.44 μM and 1.60 μM, respectively. These interesting natural product-based spiro pseudoindoxyl ketone core derivatives may be attractive for further exploration of biological activity because of the simple protocol needed to obtain them.

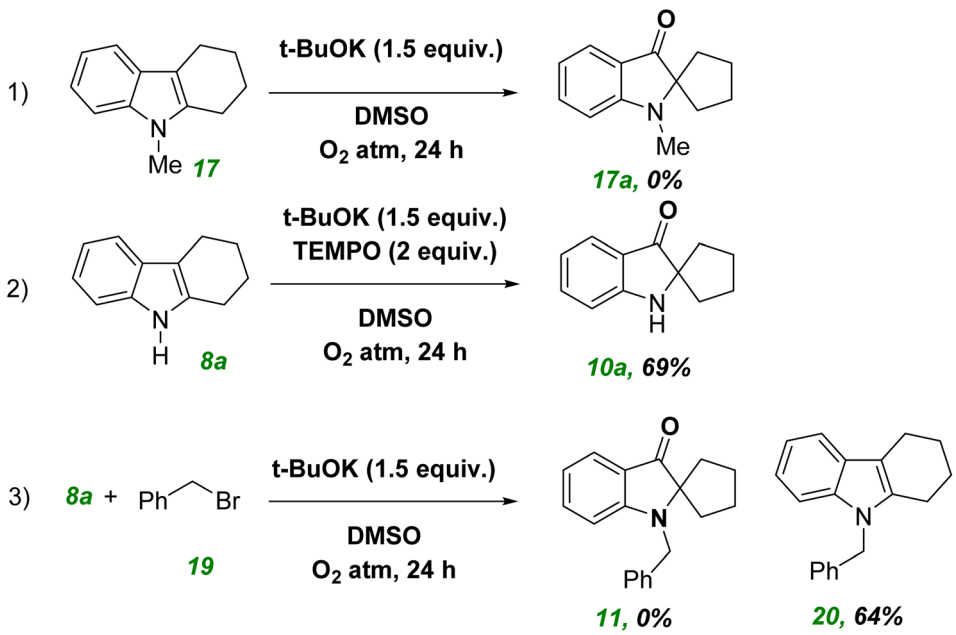

Scheme 5 Control experiment.

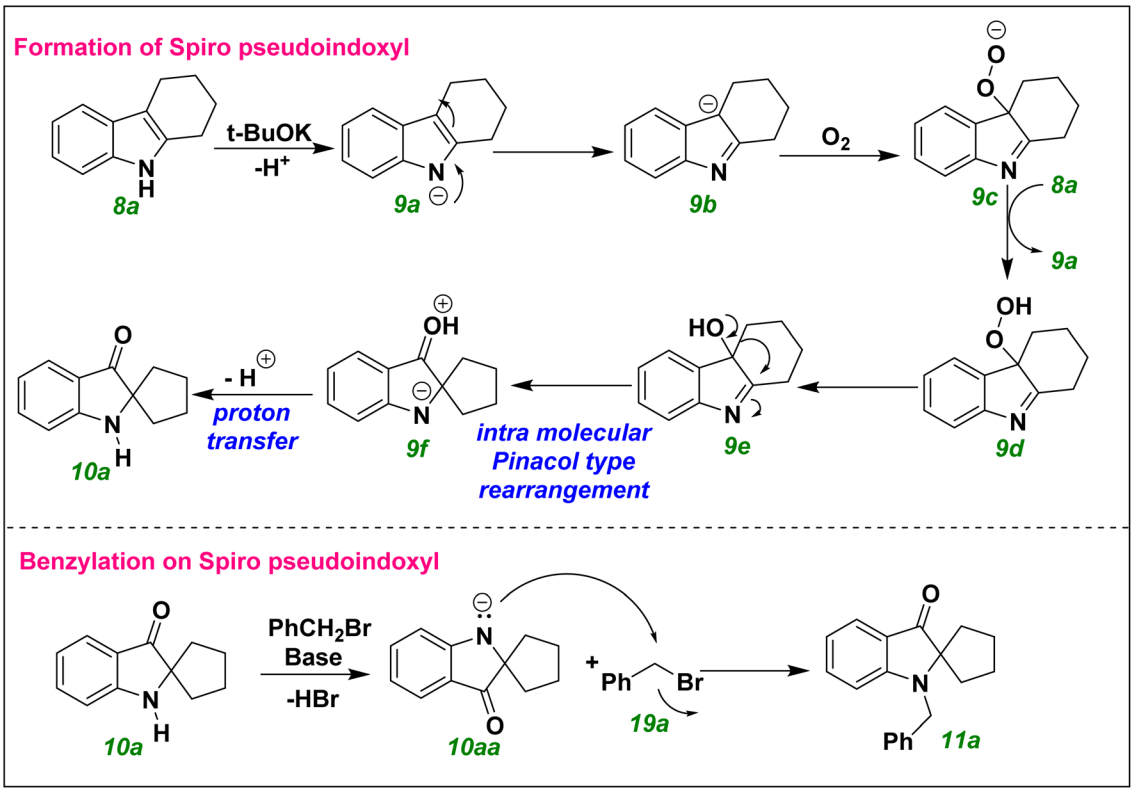

Scheme 6 Mechanistic pathway for spiro-ring formation and benzylation reaction.

Table 2 Inhibition of MAO-A and MAO-B by pseudoindoxyl compounds and their *N*-benzylated derivatives[a]

	Residual activities at 10[b] μM (%)				IC_{50} (μM)		
Compound	MAO-A	MAO-B	AChE	BChE	MAO-A	MAO-B	SI (MAO)
10a	66.86 ± 2.47	57.04 ± 2.99	76.29 ± 6.64	73.90 ± 4.90	20.78 ± 2.89	15.56 ± 2.33	1.34
10b	72.15 ± 3.58	82.16 ± 9.06	83.39 ± 1.93	73.82 ± 7.10	>40	>40	—
10c	79.09 ± 6.43	78.03 ± 5.36	100.47 ± 5.23	73.59 ± 4.50	20.17 ± 3.78	23.62 ± 3.89	0.85
10d	75.45 ± 1.29	66.95 ± 1.20	60.87 ± 4.42	76.34 ± 3.15	20.59 ± 0.49	16.54 ± 2.01	1.24
10e	68.67 ± 1.16	67.75 ± 0.76	80.16 ± 1.17	73.96 ± 2.95	30.68 ± 5.72	26.11 ± 4.15	1.18
11a	80.67 ± 0.94	61.27 ± 4.98	68.31 ± 0.51	75.90 ± 1.27	>40	12.20 ± 1.02	3.28
11b	79.56 ± 5.03	26.12 ± 2.75	80.92 ± 5.07	65.10 ± 0.74	>40	5.99 ± 0.36	6.68
11c	65.96 ± 0.11	28.99 ± 4.10	92.81 ± 8.99	59.41 ± 5.45	19.19 ± 0.048	5.76 ± 1.24	3.33
11d	62.00 ± 0.94	−16.24 ± 2.34	81.90 ± 1.22	71.19 ± 4.17	14.04 ± 0.96	2.81 ± 0.71	5.00
11e	81.33 ± 2.56	43.56 ± 5.39	99.10 ± 14.24	52.80 ± 3.25	31.06 ± 4.05	9.33 ± 1.82	3.33
11f	67.91 ± 6.53	5.22 ± 1.06	68.95 ± 0.39	72.06 ± 6.88	17.15 ± 1.14	1.44 ± 0.21	11.91
11g	73.81 ± 6.06	56.98 ± 0.00	75.50 ± 3.71	83.65 ± 1.02	24.17 ± 0.41	12.59 ± 1.41	1.92
11h	63.51 ± 5.73	2.19 ± 0.95	54.58 ± 5.23	88.43 ± 0.89	22.42 ± 0.68	1.60 ± 0.46	14.01
11i	24.12 ± 2.50	11.00 ± 0.67	68.56 ± 2.92	69.27 ± 3.68	5.58 ± 0.39	3.02 ± 0.39	1.85
11j	45.24 ± 3.37	−3.28 ± 2.80	70.21 ± 5.56	72.36 ± 9.17	8.95 ± 0.098	2.78 ± 0.60	3.22
11k	41.94 ± 4.56	60.20 ± 1.44	68.03 ± 3.68	51.41 ± 0.53	9.01 ± 0.36	14.31 ± 1.45	0.63
Toloxatone	—	—	—	—	1.646 ± 0.094	>40	<0.041
Safinamide	—	—	—	—	>40.0	0.019 ± 0.0019	>2105.26
Clorgyline	—	—	—	—	0.0079 ± 0.00094	2.43 ± 0.71	0.0033
Pargyline	—	—	—	—	2.15 ± 0.23	0.11 ± 0.011	19.55

[a] SI, selectivity index = IC_{50} (MAO-A)/IC_{50}(MAO-B). [b] A negative value means that the slope of the activity in the presence of the inhibitor was lower than that in the absence of the inhibitor (*i.e.*, control) in the continuous assay.

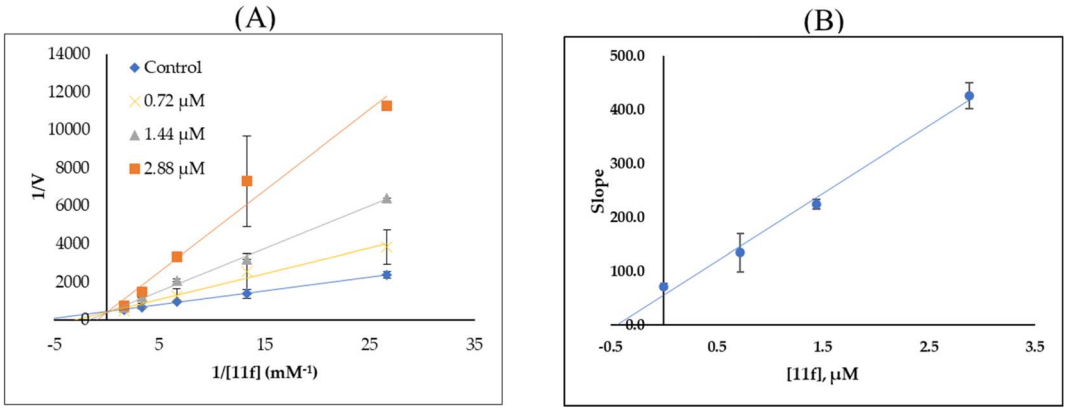

Fig. 2 Lineweaver–Burk plots for MAO-B inhibition by **11f** (A) and secondary plots (B) of the slope *vs.* inhibitor concentration.

Experimental section

General information

All reactions were undertaken in oven-dried round-bottom flasks and vials. Analytical TLC was done using F_{254} silica gel-precoated plates (Merck 60; Merck, Darmstadt, Germany). ^{1}H NMR spectra were recorded using a NMR spectrometer (600 MHz; JEOL, Tokyo, Japan) and a spectrometer (300 MHz; Bruker, Ettlingen, Germany). ^{13}C NMR spectra were recorded using a NMR spectrometer (150 MHz; JEOL) and a spectrometer (100 or 125 MHz (Bruker) using $CDCl_3$. ^{1}H NMR spectra are reported in parts per million (ppm) downfield of the internal standard (tetramethylsilane). The multiplicities are denoted as s (singlet), d (doublet), t (triplet), q (quartet), m (multiplet), or dd (doublet of doublets). The coupling constants (*J*) are reported in hertz (Hz). HRMS was undertaken using a quadrupole time of flight-micro mass spectrometer. Melting points were determined using a capillary melting-point apparatus and are uncorrected.

Materials and methods

Chemicals. Unless stated otherwise, materials and solvents were purchased from Avra, TCI, Merck, Alfa Aesar, SRL, Pure-chem, and other commercial suppliers. They were used as received. Recombinant human MAO-A, MAO-B, benzylamine, kynuramine, safinamide mesylate salt, pargyline, clorgyline, and toloxatone were purchased from MilliporeSigma (Burlington, MA, USA). Sodium phosphate (dibasic and monobasic anhydrous) was purchased from Daejung Chemicals and Metals (Siheung, Korea). Dialyzer (6–8 kDa; DiaEasy™) was purchased from BioVision (Saint Grove, MA, USA).[22]

Inhibition studies of MAO-A and MAO-B. The activities of MAO-A and MAO-B were assayed using kynuramine (0.06 mM) and benzylamine (0.30 mM), respectively, by measuring absorbance changes at 316 and 250 nm continuously, respectively. Toloxatone, clorgyline, safinamide, and pargyline were used as reference compounds. For inhibition studies, residual activities were assayed after the addition of each inhibitor at 10 μM as an

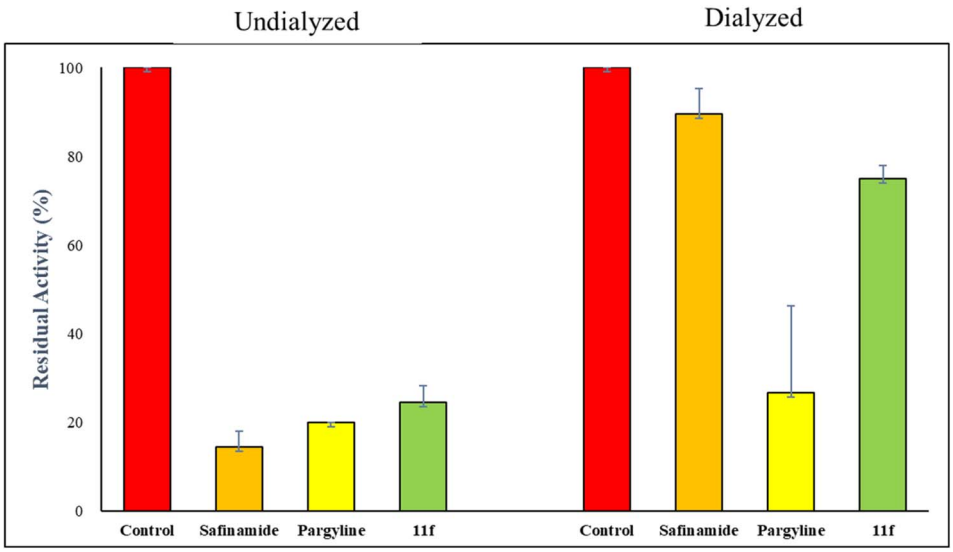

Fig. 3 Recoveries of MAO-B inhibition by **11f** using dialysis experiments. The concentration of compounds used was 2-times their IC_{50} value.

initial screening step, and then IC_{50} values were determined for potentially effective compounds using residual activity curves obtained by Prism 5 (GraphPad, San Diego, CA, USA).[23] The SI value of MAO-B was calculated as IC_{50} of MAO-A/IC_{50} of MAO-B.[24]

Enzyme kinetics. MAO-B activity was assayed at five substrate concentrations (0.0375–0.60 mM). The inhibition type of the lead compound **11f** for MAO-B was determined at three inhibitor concentrations.[25] The kinetic pattern and K_i value of enzymes were determined by comparing the Lineweaver–Burk plots and their secondary plots, respectively.[26]

Reversibility studies. The reversibility of the lead compound **11f** for MAO-B was evaluated by comparing the undialyzed and dialyzed residual activities at a concentration 2-times the IC_{50} value after pre-incubation for 30 min before measurement. Two types of reference inhibitors were used for MAO-B: safinamide mesylate (reversible inhibitor) and pargyline (non-reversible inhibitor).[27] All reference compounds were used at 2-times their IC_{50} value, 0.038 and 0.22 μM, respectively.

Conflicts of interest

There are no conflicts to declare.

Acknowledgements

S. R. sincerely thanks SERB, Government of India, New Delhi, for financial support under the SERB-Research Scientist Program (SB/SRS/2022-23/78/CS) and thanks SASTRA Deemed University for a TRR research grant. The authors gratefully acknowledge the DST-FIST grant (SR/FST/CS-I/2018/62) to SCBT and SASTRA Deemed University for providing the NMR facility. K. P. gratefully acknowledges Teaching Assistantship from SASTRA Deemed University, Thanjavur, India.

References

1 (*a*) P. S. Steyn, *Tetrahedron Lett.*, 1971, **12**, 3331; (*b*) G. Laus, *Phytother. Res.*, 2004, **18**, 259; (*c*) S.-M. Li, *Nat. Prod. Rep.*, 2010, **27**, 57; (*d*) M. E. Rateb and R. Ebel, *Nat. Prod. Rep.*, 2011, **28**, 290; (*e*) J. Sun, D. Shi, M. Ma, S. Li, S. Wang, L. Han, Y. Yang, X. Fan, J. Shi and L. He, *J. Nat. Prod.*, 2005, **68**, 915; (*f*) S. D. Pawan, P. Pitambar, V. Kumar and V. R. Chepuri, *Org. Biomol. Chem.*, 2021, **19**, 7970–7994.

2 (*a*) A. J. Hutchison and Y. Kishi, Stereospecific total synthesis of dl- austamide, *J. Am. Chem. Soc.*, 1979, **101**, 6786–6788; (*b*) R. M. Williams, T. Glinka, E. Kwast, H. Coffman and J. K. Stille, *J. Am. Chem. Soc.*, 1990, **112**, 808–821; (*c*) D. Stoermer and C. H. Heathcock, *J. Org. Chem.*, 1993, **58**, 564–568; (*d*) D. L. Boger, J. A. McKie, T. Nishi and T. Ogiku, *J. Am. Chem. Soc.*, 1996, **118**, 2301–2302; (*e*) P. S. Baran and E. J. Corey, *J. Am. Chem. Soc.*, 2002, **124**, 7904–7905; (*f*) L. A. Adams, M. W. N. Valente and R. M. Williams, *Tetrahedron*, 2006, **62**, 5195–5200; (*g*) W. Fazuo, F. Yuchun, Z. Tianjiao, Z. Min, L. Aiqun, G. Qianqun and Z. Weiming, *Tetrahedron*, 2008, **64**, 7986–7991; (*h*) J. Kim, J. S. Schneekloth Jr and E. J. Sorensen, *Chem. Sci.*, 2012, **3**, 2849–2852; (*i*) A. Váradi, G. F. Marrone, T. C. Palmer, A. Narayan, M. R. Szabó, V. Le Rouzic, S. G. Grinnell, J. J. Subrath, E. Warner, S. Kalra, A. Hunkele, J. Pagirsky, S. O. Eans, J. M. Medina, J. Xu, Y. X. Pan, A. Borics, G. W. Pasternak, J. P. McLaughlin and S. Majumdar, *J. Med. Chem.*, 2016, **59**, 8381–8397; (*j*) P. Tanguturi and J. M. Streicher, *Front. Pharmacol*, 2023, **14**, 1056402; (*k*) J. Z. Huang, Y. Ren, Y. Xu, T. Chen, T. C. Xia, Z. R. Li, J. N. Zhao, F. Hua, S. Y. Sheng and Y. Xia, *CNS Neurosci. Ther.*, 2018, **24**, 1089–1099.

3 (*a*) R. M. Williams and R. J. Cox, *Acc. Chem. Res.*, 2003, **36**, 127–139; (*b*) K. He, S. Valcic, B. N. Timmermann and G. Montenegro, *Int. J. Pharmacogn.*, 1997, **35**, 215–217; (*c*) A. D. Borthwick, *Chem. Rev.*, 2012, **112**, 3641–3716.

4 (*a*) J. H. Lee, J. H. So, J. H. Jeon, E. B. Choi, Y. R. Lee, Y. T. Chang, C. H. Kim, M. A. Bae and J. H. Ahn, *Chem. Commun.*, 2011, **47**, 7500–7502; (*b*) V. András, M. Gina, C. P. Travis, N. Ankita, R. S. Marton, R. Valerie Le, G. G. Steven, J. S. Joan, W. Evelyn, K. Sanjay, H. Amanda, P. Jeremy, O. E. Shainnel, M. M. Jessica, X. Jin, P. Ying-Xian, B. Attila, P. Gavril, P. W. Gavril, P. M. Jay and M. Susruta, *J. Med. Chem.*, 2016, **59**, 8381–8397.

5 P. N. Wyrembak and A. D. Hamilton, *J. Am. Chem. Soc.*, 2009, **131**, 4566–4567.

6 S. Matsumoto, D. Samata, M. Akazome and K. Ogura, *Tetrahedron Lett.*, 2009, **50**, 111–114.

7 H. Chen, H. Shang, Y. Liu, R. Guo and W. Lin, *Adv. Funct. Mater.*, 2016, **26**, 8128–8136.

8 (*a*) E. F. Khusnutdinova, O. B. Kazakova, A. N. Lobov, O. S. Kukovinets, K. Y. Suponitsky, C. B. Meyers and M. N. Prichard, *Org. Biomol. Chem.*, 2019, **17**, 585–597; (*b*) R. Güller and H. J. Borschberg, *Tetrahedron: Asymmetry*, 1992, **3**, 1197–1204; (*c*) X. Zhang and C. S. Foote, *J. Am. Chem. Soc.*, 1993, **115**, 8867–8868; (*d*) Y. Liu and W. W. McWhorter, *J. Org. Chem.*, 2003, **68**, 2618–2622; (*e*) Y. Liu and W. W. McWhorter, *J. Am. Chem. Soc.*, 2003, **125**, 4240–4252; (*f*) M. Movassaghi, M. A. Schmidt and J. A. Ashenhurst, *Org. Lett.*, 2008, **10**, 4009–4012; (*g*) K. Higuchi, Y. Sato, S. Kojima, M. Tsuchimochi, K. Sugiura, M. Hatori and T. Kawasaki, *Tetrahedron*, 2010, **66**, 1236–1243; (*h*) Q. Yin and S.-L. You, *Chem. Sci.*, 2011, **2**, 1344–1348; (*i*) Y.-Z. Liu, R.-L. Cheng and P.-F. Xu, *J. Org. Chem.*, 2011, **76**, 2884–2887; (*j*) W. Sun, L. Hong and R. Wang, *Chem.–Eur. J.*, 2011, **17**, 6030–6033; (*k*) A. Wetzel and F. Gagosz, *Angew. Chem., Int. Ed.*, 2011, **50**, 7354–7358; (*l*) F. Kolundzic, M. N. Noshi, M. Tjandra, M. Movassaghi and S. J. Miller, *J. Am. Chem. Soc.*, 2011, **133**, 9104–9111.

9 (*a*) C. Guo, M. Schedler, C. G. Daniliuc and F. Glorius, *Angew. Chem., Int. Ed.*, 2014, **53**, 10232–10236; (*b*) J. S. Schneekloth Jr, J. Kim and E. J. Sorensen, *Tetrahedron*, 2009, **65**, 3096–3101; (*c*) V. G. Correia, J. C. Abreu, C. A. Barata and L. H. Andrade, *Org. Lett.*, 2017, **19**, 1060–1063; (*d*) V. Pirovano, E. Brambilla, S. Rizzato, G. Abbiati, M. Bozzi and E. Rossi, *J. Org. Chem.*, 2019, **84**, 5150–5166; (*e*) W. Fu and Q. Song, *Org. Lett.*, 2018, **20**, 393–396; (*f*) W. Ding, Q. Q. Zhou, J. Xuan, T. R. Li, L. Q. Lu and W. J. Xiao, *Tetrahedron Lett.*, 2014, **55**, 4648–4652.

10 Bhawna, A. Kumar, M. Bhatia, A. Kapoor, P. Kumar and S. Kumar, *Eur. J. Med. Chem.*, 2022, **242**, 114655.
11 S. Kumar, A. S. Nair, V. Bhashkar, S. T. Sudevan, V. P. Koyiparambath, A. Khames, M. A. Abdelgawad and B. Mathew, *ACS Omega*, 2021, **6**, 23399–23411.
12 P. Guglielmi, S. Carradori, I. D'Agostino, C. Campestre and J. P. Petzer, *Expert Opin. Ther. Pat.*, 2022, **32**, 849–883.
13 R. K. P. Tripathi and S. R. Ayyannan, *Med. Res. Rev.*, 2019, **39**, 1603–1706.
14 Y. Y. Tan, P. Jenner and S. D. Chen, *J. Parkinson's Dis.*, 2022, **12**, 477–493.
15 M. Alborghetti and F. Nicoletti, *Curr. Neuropharmacol.*, 2019, **17**, 861–873.
16 C. D. Binde, I. F. Tvete, J. I. Gåsemyr, B. Natvig and M. Klemp, *Eur. J. Clin. Pharmacol.*, 2020, **76**, 1731–1743.
17 P. Riederer and T. Müller, *J. Neural Transm.*, 2018, **125**, 1751–1757.
18 N. T. Tzvetkov, S. Hinz, P. Küppers, M. Gastreich and C. E. Müller, *J. Med. Chem.*, 2014, **57**, 6679–6703.
19 A. Elkamhawy, S. Paik, H. J. Kim, J. H. Park, A. M. Londhe, K. Lee, A. N. Pae, K. D. Park and E. J. Roh, *J. Enzyme Inhib. Med. Chem.*, 2020, **35**, 1568–1580.
20 R. Sasidharan, S. L. Manju, G. Uçar, I. Baysal and B. Mathew B, *Arch. Pharm.*, 2016, **349**, 627–637.
21 (*a*) C. U. Rogers and B. B. Corson, *J. Am. Chem. Soc.*, 1947, **69**, 2910–2911; (*b*) J. Chen and Y. Hu, *Synth. Commun.*, 2006, **36**, 1485–1494; (*c*) M. C. da Silva Mendes, B. R. Fazolo, J. M. de Souza, L. G. de Vasconcelos, P. T. de Sousa, E. L. Dall'Oglio, M. A. Soares, O. M. Sampaio and L. C. C. Vieira, *Photochem. Photobiol. Sci.*, 2019, **18**, 1350–1358.
22 J. M. Oh, T. M. Rangarajan, R. Chaudhary, R. P. Singh, M. Singh, R. P. Singh, A. R. Tondo, N. Gambacorta, O. Nicolotti, B. Mathew and H. Kim, *Molecules*, 2020, **25**, 2356.
23 J. M. Oh, Y. Kang, J. H. Hwang, J. H. Park, W. H. Shin, S. K. Mun, J. U. Lee, S. T. Yee and H. Kim, *Int. J. Biol. Macromol.*, 2022, **217**, 910–921.
24 S. C. Baek, M. H. Park, H. W. Ryu, J. P. Lee, M. G. Kang, D. Park, C. M. Park, S. R. Oh and H. Kim, *Bioorg. Chem.*, 2019, **83**, 317–325.
25 S. C. Baek, H. W. Lee, H. W. Ryu, M. G. Kang, D. Park, S. H. Kim, M. L. Cho, S. R. Oh and H. Kim, *Bioorg. Med. Chem. Lett.*, 2018, **28**, 584–588.
26 J. M. Oh, H. J. Jang, W. J. Kim, M. G. Kang, S. C. Baek, J. P. Lee, D. Park, S. R. Oh and H. Kim, *Int. J. Biol. Macromol.*, 2020, **151**, 441–448.
27 H. W. Lee, H. W. Ryu, M. G. Kang, D. Park, S. R. Oh and H. Kim, *Bioorg. Med. Chem. Lett.*, 2016, **26**, 4714–4719.
28 B. Moreshwar, S. Yogesh, M. Shreyas, H. Anirban and G. Boopathy, *Org. Lett.*, 2017, **19**, 3628–3631.